11-2019

Spatial Multiplexing of Squeezed Light by Coherence Diffusion

Jian Sun

(...)

Eugeniy E. Mikhailov
William & Mary, eemikh@wm.edu

Irina Novikova
William & Mary, inovikova@physics.wm.edu

et al.

Recommended Citation

Sun, Jian; (...); Mikhailov, Eugeniy E.; Novikova, Irina; and et al., Spatial Multiplexing of Squeezed Light by Coherence Diffusion (2019). *Physical Review Letters*, 123(20).
https://doi.org/10.1103/PhysRevLett.123.203604

Spatial Multiplexing of Squeezed Light by Coherence Diffusion

Jian Sun,[1] Xichang Zhang,[1] Weizhi Qu,[1] Eugeniy E. Mikhailov,[2] Irina Novikova,[2] Heng Shen,[3,*] and Yanhong Xiao[1,†]
[1]Department of Physics, State Key Laboratory of Surface Physics and Key Laboratory of Micro and Nano Photonic Structures (Ministry of Education), Fudan University, Shanghai 200433, China
[2]Department of Physics, College of William and Mary, Williamsburg, Virginia 23185, USA
[3]Clarendon Laboratory, University of Oxford, Parks Road, Oxford OX1 3PU, United Kingdom

(Received 20 December 2018; published 14 November 2019)

Spatially splitting nonclassical light beams is in principle prohibited due to noise contamination during beam splitting. We propose a platform based on thermal motion of atoms to realize spatial multiplexing of squeezed light. Light channels of separate spatial modes in an antirelaxation coated vapor cell share the same long-lived atomic coherence jointly created by all channels through the coherent diffusion of atoms, which in turn enhances the individual channel's nonlinear process responsible for light squeezing. Consequently, it behaves as squeezed light in one optical channel transferring to other distant channels even with laser powers below the threshold for squeezed light generation. An array of squeezed light beams is created with low laser power ∼ milliwatt. This approach holds great promise for applications in a multinode quantum network and quantum enhanced technologies such as quantum imaging and sensing.

DOI: 10.1103/PhysRevLett.123.203604

A coherent optical field can be easily split into two identical beams using a simple glass or crystal beam splitter. However, such an operation for a quantum state of light is nontrivial since a conventional beam splitter introduces additional vacuum noise to each of its outputs, deteriorating their quantum properties. As a consequence, when spatially separated multiple nonclassical sources are needed for, e.g., multinode quantum networks [1,2] or multipartite entanglement generation schemes [3–6], one typically has to use multiple identical sources, each including a parametric nonlinear crystal and a cavity to generate one beam of squeezed light or one photon pair. Thus, the challenge of producing scalable arrays of nonclassical light beams is of great importance both for fundamental studies of quantum optics and for practical applications in quantum communications and quantum imaging with high spatial resolution [7–9].

In this Letter, we propose and experimentally demonstrate the possibility of generating spatially multiplexed squeezed light using a thermal atomic ensemble interacting with multiple spatially separated laser beams (channels). The proposed method takes advantage of the transport of long-lived atomic coherence in an antirelaxation coated vapor cell to enhance the nonlinear atom-light interaction and boost squeezing production in each channel, as multiple pump beams serve as the mutual optical pumping or state-preparation sources for each other. Strikingly, such arrangements allow for efficient generation of squeezing in an optical channel with the pump laser power below the single-beam squeezing threshold. Previously, such coherence transport has been used to demonstrate anti-parity-time symmetric optics [10] and a slow light beam splitter [11] for classical light, and this is the first (up to our knowledge) demonstration of spatial multiplexing capabilities for quantum optical beams.

To model the light-atom interaction resulting in squeezing generation, we consider a double-Λ scheme, in which two common excited states are connected to two ground states. The long-lived ground-state coherence results in strong enhancement of nonlinear interactions [12,13], reducing the power requirements and enabling efficient generation of both a few photon and continuous variable quantum optical states without the need for an optical cavity [14,15]. In our system, we employ the coherence created between the Zeeman sublevels by the interaction with the linearly polarized pump laser field to enhance the polarization self-rotation (PSR) nonlinearity, leading to quantum noise modifications in the orthogonal polarization [16]. This process can be attributed to the enhanced cross-phase modulation between the left- and right-circularly polarized components of the x-polarized pump field, interacting with the optical transitions $|1\rangle \rightarrow |3,4\rangle$ and $|2\rangle \rightarrow |3,4\rangle$ as shown in Fig. 1(b). Alternatively, such an interaction can be described as a degenerate four-wave-mixing (FWM) process where the driving laser serves as the pump twice in the FWM cycle, generating a pair of degenerate y-polarized photons, as shown in the energy diagram redrawn in the linear atomic basis. These quantum correlated y-polarized photon pairs can be treated as a quadrature-squeezed y-polarized vacuum, whereas the whole light field is in a polarization squeezed state [16–20].

In our proposal, we consider all atoms in the cell interacting with two (or more) illuminated interaction regions (channels), as shown in Fig. 1(a), with each channel

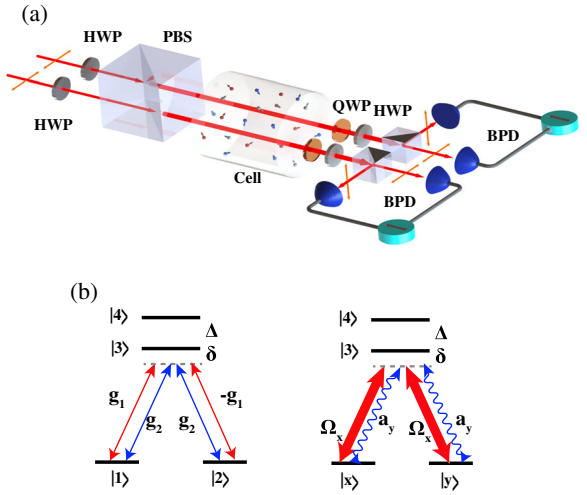

FIG. 1. Schematics for spatial multiplexing of squeezed light. (a) Experiment schematics. Two spatially separated optical channels (Ch1 and Ch2), formed by x-polarized laser beams propagating along z, interact with Rb atoms inside an antirelaxation coated vapor cell, then have their quantum fluctuations individually analyzed by balanced photodetectors (BPD) in a homodyne configuration. PBS, polarization beam splitter; HWP, half-wave plate; QWP, quarter-wave plate, used as a phase retarder here to rotate the quantum noise ellipse. (b) The double-Λ four-level interaction schemes. An x-polarized driving laser is near resonant with the $|5S_{1/2}, F = 2\rangle \rightarrow |5P_{1/2}, F' = 1, 2\rangle$ transition. In the circular basis (left diagram), the driving laser is treated as a superposition of the left- and right-circularly polarized components, driving the dipole transitions between all Zeeman sublevels of the ground state and both excited states: $|1\rangle \rightarrow |3, 4\rangle$ (with the single photon Rabi frequencies g_2, g_1) and $|2\rangle \rightarrow |3, 4\rangle$ (with Rabi frequencies g_2, $-g_1$) correspondingly. Blue arrows represent coupling between $|1, 2\rangle$ and $|3\rangle$, and red arrows represent coupling between $|1, 2\rangle$ and $|4\rangle$. The energy levels can be redrawn in the linear atomic basis (right diagram) with $|x\rangle = (1/\sqrt{2})(|1\rangle + |2\rangle)$ and $|y\rangle = (1/\sqrt{2})(|1\rangle - |2\rangle)$ to highlight the FWM description of the PSR. The x polarization drives $|x\rangle \rightarrow |3\rangle$ and $|y\rangle \rightarrow |4\rangle$, whereas the y polarization drives $|x\rangle \rightarrow |4\rangle$ and $|y\rangle \rightarrow |3\rangle$, as determined by the Clebsch-Gordan coefficients of ^{87}Rb. The detuning of laser light from the $|1\rangle \rightarrow |3\rangle$ transition is denoted as δ, and the hyperfine splitting between the two excited states is $\Delta = 814.5$ MHz. Here, $|1, 2\rangle$ refer to two Zeeman levels with the magnetic quantum number difference of 2 in all possible Λ schemes on the $F = 2$ manifold.

undergoing the above double-Λ process [21]. The spin dynamics of the moving atoms can be described by a set of coupled differential equations taking into account the spin state exchange between different regions, as well as the Langevin noise operators [22]. The effective coherence exchange between the optical channels is mediated by the atoms outside of the illuminated interaction regions, whose spin state decay slowly (coherence lifetime about 30 ms) due to the protective wall coating [25]. The optical coherence transfer between channels is negligible, as it decays within 20 ns (for ^{87}Rb). Since the laser beam diameter for each channel is much smaller than the cell diameter, atoms that are optically pumped within any optical channel quickly diffuse into the entire cell, and a steady state distribution of atomic populations and coherences within the entire cell is established with a state-preparation contribution from all channels [26,27]. Thus, it is expected that all channels will experience similar enhancement due to the common collective spin state, causing the simultaneous quantum noise reduction in all channels.

The schematic of the experiment is shown in Fig. 1. The paraffin-coated, cylindrical Pyrex cell (7.5 cm in length and 2.5 cm in diameter) contains isotopically enriched ^{87}Rb vapor, and it has a maximum operational temperature of 67 °C (limited by the coating). The cell was mounted inside a four-layer magnetic shielding with no external magnetic field applied. The output of a diode laser tuned to the $D1$ line of ^{87}Rb, passed through a polarization-maintaining optical fiber, then was separated into two or four parallel beams right after a 1-m-focal-length lens for slight focusing. All beams were passed through the same polarization beam splitter (PBS) before the cell to ensure identical polarizations. The linearly polarized input laser also played the role of the local oscillator at the output for quantum noise measurements of squeezing [28–30].

We first demonstrate the squeezing enhancement using a two-channel configuration. If only one weak pump laser beam of 1.68 mW in channel 1 (Ch1) interacts with the atoms, no squeezing is observed, as shown in Fig. 2(a). However, when another channel (Ch2) is activated, the detected quantum noise in Ch1 displays 1.37 dB squeezing below the shot noise limit at 40 kHz. More strikingly, the squeezing bandwidth of Ch1 can be increased by turning on Ch2. As shown in Fig. 2(b), when Ch1's laser power is 5.46 mW, although the 2.49 dB squeezing at 40 kHz in Ch1

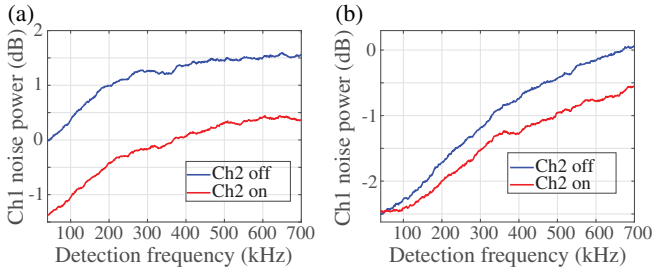

FIG. 2. Proof-of-principle two-channel squeezed light result. Measured minimal-quadrature noise spectra for both channels with the other channel on or off, obtained by a spectrum analyzer. (a) The input laser powers for Ch1 and Ch2 before the cell are 1.68 and 14.82 mW, respectively. (b) The input laser powers for Ch1 and Ch2 before the cell are 5.46 and 14.82 mW, respectively. The laser frequency is 55.2 MHz red detuned from the ^{87}Rb $D1$ line $F = 2$ to the $F' = 1$ transition. The noise power is normalized to the shot noise level. The spectrum analyzer is set to the resolution bandwidth (RBW) 10 kHz, and the video bandwidth (VBW) = 10 Hz. Each trace is averaged 200 times.

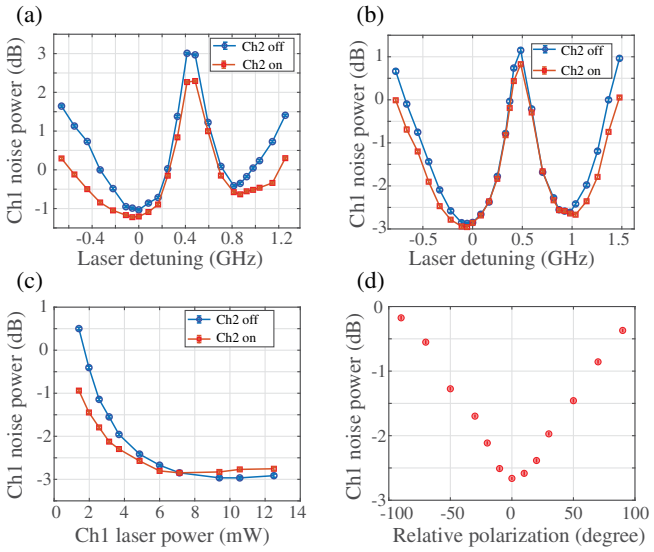

FIG. 3. Dependence on the laser detuning and laser power of the noise reduction in quadrature with minimum variance. Laser detuning dependence of the squeezed quadrature of Ch1, with and without Ch2, for (a) 2.5 mW in Ch1 and 15 mW in Ch2, and (b) 6.95 mW in Ch1 and 7.10 mW in Ch2. Zero detuning refers to resonance with the $|5S_{1/2}, F = 2\rangle \rightarrow |5P_{1/2}, F' = 1\rangle$ transition. (c) Minimum quadrature noise in Ch1's output as a function of Ch1's input laser power, with and without the Ch2 laser beam of 7.10 mW power, with the laser frequency 55.2 MHz red detuned from the $|5S_{1/2}, F = 2\rangle \rightarrow |5P_{1/2}, F' = 1\rangle$ transition. (d) Noise power reduction of Ch1 in quadrature with minimum variance, after turning on Ch2, as a function of the relative polarization angle between Ch1 and Ch2. The amount of noise power compared to the shot noise level increases as the polarization direction of the two channels offset each other. Ch1's polarization is fixed along the x direction. The laser frequency is 55.2 MHz red detuned from the ^{87}Rb $D1$ line $F = 2$ to the $F' = 1$ transition. The laser powers of Ch1 and Ch2 before the cell are 6 and 4.42 mW, respectively. Each data point is measured at the detection frequency 50 kHz and is averaged 100 times.

cannot be further increased by Ch2 due to saturation, squeezing at higher frequency can be still increased, resulting in a larger squeezing bandwidth.

To fully characterize the effect of the remote laser beam on the noise reduction, we investigate the dependence of quantum noise on the laser power, detuning and polarization. Figures 3(a) and 3(b) show the measured minimum quadrature noise for each laser frequency, as the laser frequency was scanned across the $|5S_{1/2}, F = 2\rangle \rightarrow |5P_{1/2}, F' = 1, 2\rangle$ transitions. As seen in Fig. 3(a), for the relatively low laser power of Ch1 (2.5 mW), noise reduction was observed across the whole scanning range when Ch2 is on, but with more noise reduction off resonance than near resonance. With higher power in Ch1 and lower power in Ch2 [Fig. 3(b)], the overall noise reduction effect is less pronounced when Ch2 is on, even though the overall squeezing is stronger. The reduced squeezing enhancement at higher laser power in the measurement channel can be explained by the more pronounced saturation effects occurring at higher laser powers and smaller laser detunings. To verify that, we measure the quantum noise reduction in Ch1 at different laser powers with and without a Ch2 beam with fixed power of 7.10 mW under the near-resonance regime. As expected, the amount of noise reduction decreases at higher power, as shown in Fig. 3(c). A similar trend was also observed in the off-resonant regime but with higher saturation power. The observed saturation has three contributions. (1) Closer to resonance or at higher laser power, the nonlinearity and the associated ground-state coherence for FWM, as well as the degree of squeezing, all become larger at first but then reach a plateau. (2) Stronger pump fields increase the population loss into the other hyperfine ground state due to optical pumping, leading to reduced optical depth for squeezing. This effect has been reported in antirelaxation coated cells in the slow light studies [31]. (3) Spontaneous decay of the excited states reduces the ground-state coherence and increases noise in the quantum light components. Such an influence is also stronger for the higher laser power and near-resonance regime. The third effect was observed when injecting an additional repump light to collect the atoms decaying to the other hyperfine state, i.e., $|5S_{1/2}, F = 1\rangle$, and to drive them back to $|5S_{1/2}, F = 2\rangle$. It is found that the repumper is helpful in achieving a higher degree of squeezing for medium laser power and lower temperature, as illustrated in Fig. S6 of the Supplemental Material [22] and also for a more detuned case. However, we found that the repumper does not improve squeezing when the laser parameters and cell temperature are already optimized for highest squeezing level, i.e., the higher laser power, near-resonance, and higher temperature case. This indicates that the population loss is not the dominant factor of saturation in the high-squeezing regime, and instead it is the noise associated with the spontaneous emission of the excited state. All of the above analysis and observation has been qualitatively reproduced by our numerical simulation [22].

One important requirement for this scheme is that all channels create in-phase atomic coherence. For instance, the measured noise reduction in Ch1 is affected if we vary its laser field polarization direction with respect to that of Ch2, as this changes the relative phase of the ground-state coherences prepared in the two channels, as illustrated by the circular basis diagram in Fig. 1(b). Intuitively, the interaction closely resembles a classic electromagnetically induced transparency when the laser is tuned near the resonance. In this case, the resulting Zeeman coherence bears the relative phase of the two circular light components in each channel. Thus, if the polarizations of the pump fields in two channels are different, their contributions to the collective atomic coherence will interfere destructively due to the difference in their relative phases. Figure 3(d) illustrate this effect by showing the quick deterioration of the quantum noise reduction at higher

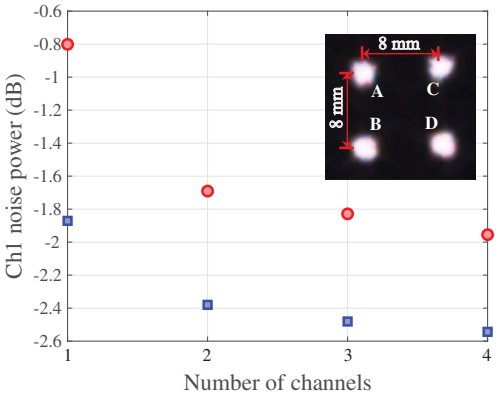

FIG. 4. 2×2 array of squeezed light. Noise power of channel D with the presence of different numbers of channels. (Inset) The spatial mapping of 2×2 parallel laser beams taken by a CCD. The distance between two adjacent beams is 8 mm. Red dots, the laser power of each channel before the cell is 2.56 mW and the laser frequency is 55.2 MHz red detuned from the ^{87}Rb $D1$ line $F = 2$ to the $F' = 1$ transition; blue dots, the laser power of each channel before the cell is 4.62 mW, and the laser frequency is 110.4 MHz red detuned from the ^{87}Rb $D1$ line $F = 2$ to the $F' = 1$ transition. The detection frequency is 50 kHz, and the noise power is relative to the shot noise level (0 dB level). The spectrum analyzer settings are RBW = 10 kHz, VBW = 10 Hz.

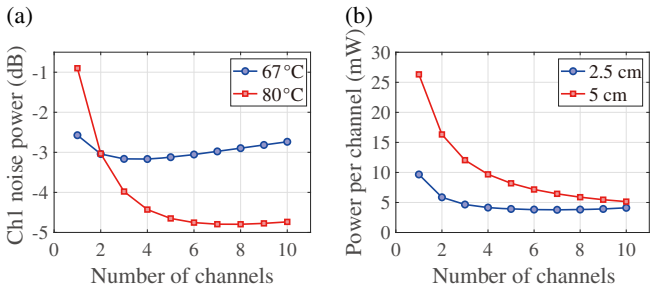

FIG. 5. Numerical results for the squeezed quadrature noise power and laser power needed in the squeezed light array. (a) Squeezed quadrature noise power as a function of channel number at 67 °C and 80 °C. The laser power in each channel is fixed at 3.5 mW. (b) Laser power needed in each channel to observe 5 dB squeezing vs the number of channels in cells with different diameters at 80 °C. The laser is 110 MHz red detuned from the $|5S_{1/2}, F = 2\rangle$ to $|5P_{1/2}, F' = 1\rangle$ transition, and the detection frequency is set at 50 kHz. The noise power is normalized to the shot noise level (0 dB level).

relative polarization angle due to reduced average coherence in the cell.

Thanks to the key advantage of the discussed squeezing multiplexing being motional coherence averaging, it is natural to extend the one-dimensional two-channel results, discussed above, to a two-dimensional (2D) configuration. We investigate the enhancement of squeezed light by distant channels in a 2×2 array, and we demonstrate a 2D array of squeezed light with low laser power as depicted in Fig. 4. For example, with a relatively low 2.56 mW of near-resonant laser power per channel, we measured only a 0.8 dB squeezing level for a single illuminated channel. However, as more channels were switched on, the measured squeezing level steadily increased to 2 dB. At a higher laser power of 4.62 mW per individual channel, the even higher squeezing level of about 2.54 dB was reached in each channel with the laser detuned a little farther from the transition to avoid detrimental saturation effects. It can be also seen that, to reach similar squeezing, the laser power per channel in the array is less than that required in the single-channel case, as shown in Figs 3(a)–3(c).

To explore the scalability of the proposed scheme, we numerically modeled a ten-channel configuration. Such a large array input can be generated by an acousto-optic deflector. As shown in Fig. 5(a), the degree of squeezing in all channels increases with the number of channels, and near 5 dB squeezing in each channel can be realized with only about 3.5 mW of pump power per channel, in a cell with a higher optical depth (equivalent to a temperature of 80 °C) that can be reached either with a longer cell or with alternative choice of high-temperature-resistant anti-relaxation coating [32]. Simulation results in Fig. 5(b) predict that increasing the number of channels will help realize a spatially multiplexed array of squeezed light with lower laser power per channel. For a fixed target squeezing level [set at 5 dB in Fig. 5(b)], the required laser power per channel reduces even faster if the diameter of the cell increases, as a larger unilluminated volume reduces the unwanted saturation effects more efficiently by motional averaging. Our model also predicts that under these conditions we should be able to achieve the highest level of squeezing at the lower detection frequencies [22], making it particularly useful for detecting biological, geological, and other signals at the subkilohertz range.

To our knowledge, the achieved 2.5 dB squeezing (3.2 dB after loss correction) of each beam in our array and the 3 dB squeezing for a single-beam case are the record-high values for PSR squeezing in a coated cell. These values are comparable with the highest single-channel polarization squeezing level in atomic vapor of about 3 dB [30], measured in an uncoated cell heated to 73 °C and with laser power 30 mW, but here less laser power and a lower atomic cell temperature are required. We deem 3 dB to be the minimal squeezing level required for the implementation of several quantum information protocols [30]. However, further improvements in our scheme are possible by increasing the effective optical depth. In addition, engineering of the spatial mode of the light involved in this scheme may further enhance squeezing [33]. With such improvements implemented, the performance of the multichannel squeezed light array should reach a squeezing level exceeding 5 dB in each channel.

Our demonstration of spatially multiplexed squeezed light provides a scalable way to produce multiple squeezed

light beams, which would be challenging for nonlinear systems requiring external cavities. Such a squeezed light array can be applied in quantum imaging and sensing [7], a quantum network with more nodes [1], and multipartite entanglement studies [5]. Although in this demonstration we focused on the continuous variable regime, our scheme should be capable of operating in the discrete variable regime, i.e., to generate arrays of entangled photon pairs, based on the recent demonstrations in a similar coated cell using hyperfine ground-state coherence [15]. Furthermore, it is possible to make the beams in the array correlate with each other at a quantum level, if a proper light configuration is used, as proposed in Ref. [34]. This would allow the future realization of entangled light arrays and investigations of nonlinear photon-photon interactions [35] mediated by flying atoms. This strategy can be extended to other systems such as trapped ion ones where the spin degree of freedom of the ions are coupled via phonon-mediated long-range interactions induced by laser forces [36–38].

We thank Eugene S. Polzik for the fruitful discussions, and Yanqiang Guo for drawing the experiment schematics. This work is supported by the National Key Research Program of China under Grants No. 2016YFA0302000 and No. 2017YFA0304204, and the NNSFC under Grants No. 61675047 and No. 91636107. H. S. acknowledges the financial support from the Royal Society Newton International Fellowship (NF170876) of the UK.

*heng.shen@physics.ox.ac.uk
†yxiao@fudan.edu.cn

[1] H. J. Kimble, Nature (London) **453**, 1023 (2008).
[2] Z. Yan, L. Wu, X. Jia, Y. Liu, R. Deng, S. Li, H. Wang, C. Xie, and K. Peng, Nat. Commun. **8**, 718 (2017).
[3] X. Su, A. Tan, X. Jia, J. Zhang, C. Xie, and K. Peng, Phys. Rev. Lett. **98**, 070502 (2007).
[4] R. Ukai, S. Yokoyama, J.-i. Yoshikawa, P. van Loock, and A. Furusawa, Phys. Rev. Lett. **107**, 250501 (2011).
[5] S. Armstrong, M. Wang, R. Y. Teh, Q. Gong, Q. He, J. Janousek, H.-A. Bachor, M. D. Reid, and P. K. Lam, Nat. Phys. **11**, 167 (2015).
[6] M. Chen, N. C. Menicucci, and O. Pfister, Phys. Rev. Lett. **112**, 120505 (2014).
[7] M. A. Taylor, J. Janousek, V. Daria, J. Knittel, B. Hage, H.-A. Bachor, and W. P. Bowen, Nat. Photonics **7**, 229 (2013).
[8] D. Budker and M. Romalis, Nat. Phys. **3**, 227 (2007).
[9] V. Giovannetti, S. Lloyd, and L. Maccone, Nat. Photonics **5**, 222 (2011).
[10] P. Peng, W. Cao, C. Shen, W. Qu, J. Wen, L. Jiang, and Y. Xiao, Nat. Phys. **12**, 1139 (2016).
[11] Y. Xiao, M. Klein, M. Hohensee, L. Jiang, D. F. Phillips, M. D. Lukin, and R. L. Walsworth, Phys. Rev. Lett. **101**, 043601 (2008).
[12] K. Hammerer, A. S. Sørensen, and E. S. Polzik, Rev. Mod. Phys. **82**, 1041 (2010).
[13] D. Budker, W. Gawlik, D. F. Kimball, S. M. Rochester, V. V. Yashchuk, and A. Weis, Rev. Mod. Phys. **74**, 1153 (2002).
[14] C. F. McCormick, V. Boyer, E. Arimondo, and P. D. Lett, Opt. Lett. **32**, 178 (2007).
[15] C. Shu, P. Chen, T. K. A. Chow, L. Zhu, Y. Xiao, M. M. T. Loy, and S. Du, Nat. Commun. **7**, 12783 (2016).
[16] A. B. Matsko, I. Novikova, G. R. Welch, D. Budker, D. F. Kimball, and S. M. Rochester, Phys. Rev. A **66**, 043815 (2002).
[17] J. Ries, B. Brezger, and A. I. Lvovsky, Phys. Rev. A **68**, 025801 (2003).
[18] S. R. de Echaniz, M. Koschorreck, M. Napolitano, M. Kubasik, and M. W. Mitchell, Phys. Rev. A **77**, 032316 (2008).
[19] W. Wasilewski, T. Fernholz, K. Jensen, L. S. Madsen, H. Krauter, C. Muschik, and E. S. Polzik, Opt. Express **17**, 14444 (2009).
[20] I. H. Agha, G. Messin, and P. Grangier, Opt. Express **18**, 4198 (2010).
[21] S. M. Rochester, Ph.D. thesis, University of California, Berkeley, 2010.
[22] See Supplemental Material at http://link.aps.org/supplemental/10.1103/PhysRevLett.123.203604, which includes Refs. [23,24], for details on the numerical model and extended experiment results on the effects of the repumper.
[23] Q. Glorieux, R. Dubessy, S. Guibal, L. Guidoni, J.-P. Likforman, T. Coudreau, and E. Arimondo, Phys. Rev. A **82**, 033819 (2010).
[24] L. Davidovich, Rev. Mod. Phys. **68**, 127 (1996).
[25] M. V. Balabas, T. Karaulanov, M. P. Ledbetter, and D. Budker, Phys. Rev. Lett. **105**, 070801 (2010).
[26] J. Borregaard, M. Zugenmaier, J. M. Petersen, H. Shen, G. Vasilakis, K. Jensen, E. S. Polzik, and A. S. Sørensen, Nat. Commun. **7**, 11356 (2016).
[27] O. Firstenberg, M. Shuker, A. Ron, and N. Davidson, Rev. Mod. Phys. **85**, 941 (2013).
[28] A. Lezama, P. Valente, H. Failache, M. Martinelli, and P. Nussenzveig, Phys. Rev. A **77**, 013806 (2008).
[29] E. E. Mikhailov and I. Novikova, Opt. Lett. **33**, 1213 (2008).
[30] S. Barreiro, P. Valente, H. Failache, and A. Lezama, Phys. Rev. A **84**, 033851 (2011).
[31] I. Novikova, R. L. Walsworth, and Y. Xiao, Laser Photonics Rev. **6**, 333 (2012).
[32] S. J. Seltzer and M. V. Romalis, J. Appl. Phys. **106**, 114905 (2009).
[33] M. Zhang, R. N. Lanning, Z. Xiao, J. P. Dowling, I. Novikova, and E. E. Mikhailov, Phys. Rev. A **93**, 013853 (2016).
[34] W. Cao, X. Lu, X. Meng, J. Sun, H. Shen, and Y. Xiao, arXiv:1903.12213.
[35] D. E. Chang, V. Vuletić, and M. D. Lukin, Nat. Photonics **8**, 685 (2014).
[36] P. Jurcevic, H. Shen, P. Hauke, C. Maier, T. Brydges, C. Hempel, B. P. Lanyon, M. Heyl, R. Blatt, and C. F. Roos, Phys. Rev. Lett. **119**, 080501 (2017).
[37] J. Zhang, G. Pagano, P. W. Hess, A. Kyprianidis, P. Becker, H. Kaplan, A. V. Gorshkov, Z.-X. Gong, and C. Monroe, Nature (London) **551**, 601 (2017).
[38] A. S. Sørensen and K. Mølmer, Phys. Rev. Lett. **82**, 1971 (1999).